1st Pan-American Congress on Computational Mechanics - PANACM 2015
XI Argentine Congress on Computational Mechanics - MECOM 2015
S. Idelsohn, V. Sonzogni, A. Coutinho, M. Cruchaga, A. Lew & M. Cerrolaza (Eds)

A VARIATIONAL FLUX RECOVERY APPROACH FOR ELASTODYNAMICS PROBLEMS WITH INTERFACES

PAVEL BOCHEV[1] AND PAUL KUBERRY[1]

[1] Computational Mathematics,
Sandia National Laboratories *, Mail Stop 1320
Albuquerque, New Mexico, 87185-1320
{pbboche, pakuber}@sandia.gov

Key words: Linear elastodynamics, material interface, partitioned solution.

Abstract. We present a new explicit algorithm for linear elastodynamic problems with material interfaces. The method discretizes the governing equations independently on each material subdomain and then connects them by exchanging forces and masses across the material interface. Variational flux recovery techniques provide the force and mass approximations. The new algorithm has attractive computational properties. It allows different discretizations on each material subdomain and enables partitioned solution of the discretized equations. The method passes a linear patch test and recovers the solution of a monolithic discretization of the governing equations when interface grids match.

1 INTRODUCTION

This paper focuses on the numerical solution of elastodynamic problems with interfaces. Such problems arise in multiple modeling and simulation contexts involving elastic bodies with discontinuous material properties. We present a new explicit scheme for such problems, which uses variational flux recovery techniques [2] to enable partitioned solution of the interface problem. Restriction of the governing equations to material subdomain yields boundary value problems linked through unknown interface traction. Approximation of the latter by variational recovery techniques decouples the subdomain problems.

The resulting algorithm has some attractive computational properties. It allows the use of different discretizations on each material subdomain and enables partitioned solution of the discretized equations. This makes it possible to also use the algorithm as a coupling tool for different codes operating in different material regions. The method passes a

*Sandia National Laboratories is a multi-program laboratory managed and operated by Sandia Corporation, a wholly owned subsidiary of Lockheed Martin Corporation, for the U.S. Department of Energy's National Nuclear Security Administration under contract DE-AC04-94AL85000.

linear patch test and recovers the solution of a monolithic discretization of the governing equations when interface grids match.

To present the method it suffices to consider small displacements and linear elastic models. Our main focus is on enabling explicit solution of the elastodynamic problem by solving independent problems on each material subdomain. Thus, we restrict attention to subdomain partitions with non-matching but spatially coincident interface grids. This is in contrast to many of the existing works on elliptic problems with interfaces, which focus primarily on capturing weak and strong discontinuities of the solution on unfitted grids. Such methods often combine Nitsche's method with extended finite elements [1, 3, 4], or define a suitable modified or enriched basis set on cut elements [5, 6].

2 NOTATIONS

We consider a bounded region $\Omega \in \mathbf{R}^d$, $d = 2, 3$ with a material interface σ. The interface splits Ω into non-overlapping subdomains Ω_1 and Ω_2 with Dirichlet boundaries $\Gamma_i = \partial\Omega_i/\sigma$, $i = 1, 2$. We assume that the interface unit normal $\boldsymbol{n}_\sigma$ coincides with the outer unit normal to $\partial\Omega_1$. The Sobolev space for the displacements on Ω_i is $\mathbf{H}(\Omega_i)$ and $\mathbf{H}_{\Gamma_i}(\Omega_i)$ is its subspace of functions that vanish on Γ_i. Each subdomain is endowed with a finite element partition Ω_i^h. The set of all mesh vertices $\{\boldsymbol{x}_{i,k}\}$ is $V(\Omega_i^h)$ and $V(\breve{\Omega}_i^h)$ are the interior mesh vertices. The subdomain partitions induce finite element partitions σ_1^h and σ_2^h of the interface σ, which are not required to match but are assumed to be spatially coincident. The set $V(\sigma_i^h)$ contains the vertices of the interface mesh σ_i^h.

S_i^h is a conforming finite element subspace of $\mathbf{H}(\Omega_i)$, defined on the mesh Ω_i^h and equipped with a standard Lagrangian basis $\{N_{i,k}\}$. The *interface* part $S_{i,\sigma}^h$ is the span of all basis functions associated with $V(\sigma_i^h)$ and $S_{i,0}^h$ is the space corresponding to the interior vertices $V(\breve{\Omega}_i^h)$. $S_{i,\Gamma}^h$ is a conforming subspace of $\mathbf{H}_{\Gamma_i}(\Omega_i)$. The coefficient vector of $\boldsymbol{u}_i \in S_i^h$ is $\vec{\boldsymbol{u}}_i = (\vec{\boldsymbol{u}}_{i,\sigma}, \vec{\boldsymbol{u}}_{i,0})$ where $\vec{\boldsymbol{u}}_{i,\sigma}$ and $\vec{\boldsymbol{u}}_{i,0}$ are the interface and interior coefficients of $\boldsymbol{u}_i$, respectively, corresponding to functions $\boldsymbol{u}_{i,\sigma} \in S_{i,\sigma}^h$ and $\boldsymbol{u}_{i,0} \in S_{i,0}^h$, respectively. The operator $\Pi_1 : S_{2,\sigma}^h \mapsto S_{1,\sigma}^h$ interpolates $\boldsymbol{u}_{2,\sigma} \in S_{2,\sigma}^h$ in $S_{1,\sigma}^h$, i.e.,

$$\Pi_1(\boldsymbol{u}_{2,\sigma}) = \sum_{i \in V(\sigma_1^h)} \boldsymbol{u}_{2,\sigma}(\boldsymbol{x}_{1,i}) N_{1,i}(\boldsymbol{x}) = \sum_{i \in V(\sigma_1^h)} \Big[\sum_{k \in V(K_2 \ni \boldsymbol{x}_{1,i})} (\vec{\boldsymbol{u}}_{2,\sigma})_k N_{2,k}(\boldsymbol{x}_{1,i}) \Big] N_{1,i}(\boldsymbol{x}) \,, \quad (1)$$

where $V(K_2 \ni \boldsymbol{x}_{1,i})$ are the vertices of element $K_2 \in \sigma_2^h$ containing vertex $\boldsymbol{x}_{1,i}$ from σ_1^h. The coefficient vector of $\Pi_1(\boldsymbol{u}_{2,\sigma})$ is given by $P_1 \vec{\boldsymbol{u}}_{2,\sigma}$ where P_1 is a $|V(\sigma_1^h)| \times |V(\sigma_2^h)|$ sparse matrix. The row of this matrix corresponding to vertex $\boldsymbol{x}_{1,i}$ contains the values $N_{2,k}(\boldsymbol{x}_{1,i})$ for $k \in V(K_2 \ni \boldsymbol{x}_{1,i})$. Similar representation holds for $\Pi_2 : S_{1,\sigma}^h \mapsto S_{2,\sigma}^h$.

3 Governing equations

We write the model elastodynamic problem as a pair of governing equations

$$\left\{ \begin{array}{rcll} \ddot{\boldsymbol{u}}_i - \nabla \cdot \sigma(\boldsymbol{u}_i) & = & \mathbf{f} & \text{in } \Omega_i \times [0,T] \\ \boldsymbol{u}_i & = & \boldsymbol{g} & \text{on } \Gamma_i \times [0,T] \end{array} \right. \quad \text{and} \quad \begin{array}{rcll} \boldsymbol{u}_i(0,\boldsymbol{x}) & = & \boldsymbol{u}_0(\boldsymbol{x}) & \text{in } \Omega_i \\ \dot{\boldsymbol{u}}_i(0,\boldsymbol{x}) & = & \dot{\boldsymbol{u}}_0(\boldsymbol{x}) & \text{in } \Omega_i \end{array} \quad (2)$$

for displacements $\boldsymbol{u}_i(t, \boldsymbol{x})$, $i = 1, 2$ in Ω_i, and a pair of interface conditions

$$\boldsymbol{u}_1(\boldsymbol{x}, t) = \boldsymbol{u}_2(\boldsymbol{x}, t) \quad \text{and} \quad \sigma_1(\boldsymbol{x}, t) \cdot \boldsymbol{n}_\sigma = \sigma_2(\boldsymbol{x}, t) \cdot \boldsymbol{n}_\sigma \quad \text{on } \sigma \times [0, T] \tag{3}$$

expressing continuity of the displacement and the traction across the interface. We restrict attention to linear elastodynamic problems for which

$$\sigma(\boldsymbol{u}_i) = \lambda_i(\nabla \cdot \boldsymbol{u}_i)I + 2\mu_i\varepsilon(\boldsymbol{u}_i), \quad \varepsilon(\boldsymbol{u}_i) = \frac{1}{2}(\nabla \boldsymbol{u}_i + \nabla \boldsymbol{u}_i^T),$$

and the Lame coefficients λ_i and μ_i are allowed to have a discontinuity along σ.

4 Formulation of the method

A formal splitting of (2)–(3) into two "independent" mixed boundary value subdomain equations is the starting point in the formulation. This partitioning is formal because it imposes the unknown traction value on the interface as a Neumann boundary condition and resulting solutions satisfy a weak continuity relation in terms of an operator that is not available in closed form. Using variational flux recovery ideas we eliminate the unknown traction from the subdomain equations. In so doing we obtain two fully decoupled subdomain equations which implicitly incorporate appropriate discrete notions of the interface conditions (3).

4.1 Formal partitioning of the governing equations

Let $\boldsymbol{u}_i$, $i = 1, 2$ denote the exact solutions of (2)–(3) and

$$\gamma = \sigma_1(\boldsymbol{x}, t) \cdot \boldsymbol{n}_\sigma = \sigma_2(\boldsymbol{x}, t) \cdot \boldsymbol{n}_\sigma$$

be the corresponding exact interface traction. If γ is known exactly then the displacement $\boldsymbol{u}_i$ on Ω_i can be determined by solving the following mixed boundary value problem:

$$\left\{ \begin{array}{rcll} \ddot{\boldsymbol{u}}_i - \nabla \cdot \sigma_i &=& \mathbf{f} & \text{in } \Omega_i \times [0, T] \\ \boldsymbol{u}_i &=& \boldsymbol{g} & \text{on } \Gamma_i \times [0, T] \\ \sigma_i(\boldsymbol{x}, t) \cdot \boldsymbol{n}_\sigma &=& \gamma & \text{on } \sigma \times [0, T] \end{array} \right. \quad \text{and} \quad \begin{array}{rcll} \boldsymbol{u}_i(0, \boldsymbol{x}) &=& \boldsymbol{u}_0(\boldsymbol{x}) & \text{in } \Omega_i \\ \dot{\boldsymbol{u}}_i(0, \boldsymbol{x}) &=& \dot{\boldsymbol{u}}_0(\boldsymbol{x}) & \text{in } \Omega_i \end{array} \tag{4}$$

The exact traction γ specifics a Neumann boundary condition on σ, which closes the subdomain problems and makes it possible to solve them independently from each other. By the uniqueness of the solutions to (2)–(3) and (4) it follows that the solutions of the latter necessarily satisfy the first interface condition in (3), i.e., $\boldsymbol{u}_1 = \boldsymbol{u}_2$ on σ.

The weak form of the equations in (4) are: seek $\boldsymbol{u}_i \in \mathbf{H}(\Omega_i)$, $i = 1, 2$ such that

$$\begin{array}{l} (\ddot{\boldsymbol{u}}_1, \boldsymbol{v}_1)_{\Omega_1} + (\sigma_1, \varepsilon(\boldsymbol{v}_1))_{\Omega_1} = (\mathbf{f}, \boldsymbol{v}_1)_{\Omega_1} + \langle \gamma, \boldsymbol{v}_1 \rangle_\sigma \quad \forall \boldsymbol{v}_1 \in \mathbf{H}_{\Gamma_1}(\Omega_1) \\ (\ddot{\boldsymbol{u}}_2, \boldsymbol{v}_2)_{\Omega_2} + (\sigma_2, \varepsilon(\boldsymbol{v}_2))_{\Omega_2} = (\mathbf{f}, \boldsymbol{v}_2)_{\Omega_2} - \langle \gamma, \boldsymbol{v}_2 \rangle_\sigma \quad \forall \boldsymbol{v}_2 \in \mathbf{H}_{\Gamma_2}(\Omega_2) \end{array} . \tag{5}$$

Solutions of (5) necessarily satisfy the first interface condition in (3), i.e., $\boldsymbol{u}_1 = \boldsymbol{u}_2$ on σ.

4.2 Spatial discretization

The finite element spatial discretization of (5) is to seek $\boldsymbol{u}_i \in S_i^h \times [0,T]$, which satisfies the initial and boundary conditions in (4) and is such that

$$\begin{aligned}(\ddot{\boldsymbol{u}}_1, \boldsymbol{v}_1)_{\Omega_1} + (\sigma(\boldsymbol{u}_1), \varepsilon(\boldsymbol{v}_1))_{\Omega_1} &= (\mathbf{f}, \boldsymbol{v}_1)_{\Omega_1} + \langle \gamma, \boldsymbol{v}_1 \rangle_\sigma \quad \forall \boldsymbol{v}_1 \in S_{1,\Gamma}^h \\ (\ddot{\boldsymbol{u}}_2, \boldsymbol{v}_2)_{\Omega_2} + (\sigma(\boldsymbol{u}_1), \varepsilon(\boldsymbol{v}_2))_{\Omega_2} &= (\mathbf{f}, \boldsymbol{v}_2)_{\Omega_2} - \langle \gamma, \boldsymbol{v}_2 \rangle_\sigma \quad \forall \boldsymbol{v}_2 \in S_{2,\Gamma}^h\end{aligned} \tag{6}$$

Since in general σ_1^h and σ_2^h are non-matching finite element partitions of σ, solutions of (6) can only satisfy a "weak" notion of displacement continuity

$$\boldsymbol{u}_{1,\sigma} = \Pi_1(\boldsymbol{u})\boldsymbol{u}_{2,\sigma} \quad \text{and} \quad \boldsymbol{u}_{2,\sigma} = \Pi_2(\boldsymbol{u})\boldsymbol{u}_{1,\sigma} \tag{7}$$

where $\Pi_1(\boldsymbol{u}) : S_1^h \mapsto S_2^h$ and $\Pi_2(\boldsymbol{u}) : S_2^h \mapsto S_1^h$ are some unknown operators.

4.3 Elimination of the surface traction

The unknown interface traction γ and the weak continuity condition (7) couple the discrete subdomain equations (6). This section explains the elimination of the surface traction from the equations. We rewrite (6) in a block form corresponding to the partitioning of S_i^h into an interfacial part $S_{i,\sigma}^h$ and a zero trace part $S_{i,0}^h$, along with the appropriate weak continuity equation. This form is given by

$$\begin{cases} (\ddot{\boldsymbol{u}}_{1,\sigma}, N_{1,i})_{\Omega_1} + (\sigma(\boldsymbol{u}_1), \varepsilon(N_{1,i}))_{\Omega_1} = (\mathbf{f}, N_{1,i})_{\Omega_1} + \langle \gamma, N_{1,i} \rangle_\sigma & \forall i \in V(\sigma_1^h) \\ (\ddot{\boldsymbol{u}}_{1,0}, N_{1,i})_{\Omega_1} + (\sigma(\boldsymbol{u}_1), \varepsilon(N_{1,i}))_{\Omega_1} = (\mathbf{f}, N_{1,i})_{\Omega_1} & \forall i \in V(\breve{\Omega}_1^h) \\ \boldsymbol{u}_{1,\sigma} = \Pi_1(\boldsymbol{u})\boldsymbol{u}_{2,\sigma} \end{cases} \tag{8}$$

on the first subdomain and by

$$\begin{cases} (\ddot{\boldsymbol{u}}_{2,\sigma}, N_{2,i})_{\Omega_2} + (\sigma(\boldsymbol{u}_2), \varepsilon(N_{2,i}))_{\Omega_2} = (\mathbf{f}, N_{2,i})_{\Omega_2} - \langle \gamma, N_{2,i} \rangle_\sigma & \forall i \in V(\sigma_2^h) \\ (\ddot{\boldsymbol{u}}_{2,0}, N_{2,i})_{\Omega_2} + (\sigma(\boldsymbol{u}_2), \varepsilon(N_{2,i}))_{\Omega_2} = (\mathbf{f}, N_{2,i})_{\Omega_2} & \forall i \in V(\breve{\Omega}_2^h) \\ \boldsymbol{u}_{2,\sigma} = \Pi_2(\boldsymbol{u})\boldsymbol{u}_{1,\sigma} \end{cases} \tag{9}$$

on the second subdomain. We use (9) to eliminate the unknown traction γ from (8) and vice versa. Solving the interface equations in (9) for γ yields

$$\langle \gamma, N_{2,i} \rangle_\sigma = (\mathbf{f}, N_{2,i})_{\Omega_2} - (\sigma(\boldsymbol{u}_2), \varepsilon(N_{2,i}))_{\Omega_2} - (\ddot{\boldsymbol{u}}_{2,\sigma}, N_{2,i})_{\Omega_2} \quad \forall i \in V(\sigma_2^h). \tag{10}$$

Equation (10) defines a finite element approximation $\gamma_2(\ddot{\boldsymbol{u}}_{2,\sigma}, \boldsymbol{u}_2) \in S_{2,\sigma}^h$ of the interface traction in terms of $\ddot{\boldsymbol{u}}_{2,\sigma}$ and $\boldsymbol{u}_2$. It can be interpreted as variational recovery [2] of γ from a finite element solution. Then we approximate γ in (8) by the interpolant $\Pi_1\gamma_2 \in S_{1,\sigma}^h$. This yields the following system of equations on the first subdomain:

$$\begin{cases} (\ddot{\boldsymbol{u}}_{1,\sigma}, N_{1,i})_{\Omega_1} + (\sigma(\boldsymbol{u}_1), \varepsilon(N_{1,i}))_{\Omega_1} = (\mathbf{f}, N_{1,i})_{\Omega_1} + \langle \Pi_1\gamma_2(\ddot{\boldsymbol{u}}_{2,\sigma}, \boldsymbol{u}_2), N_{1,i} \rangle_\sigma & \forall i \in V(\sigma_1^h) \\ (\ddot{\boldsymbol{u}}_{1,0}, N_{1,i})_{\Omega_1} + (\sigma(\boldsymbol{u}_1), \varepsilon(N_{1,i}))_{\Omega_1} = (\mathbf{f}, N_{1,i})_{\Omega_1} & \forall i \in V(\breve{\Omega}_1^h) \\ \boldsymbol{u}_{1,\sigma} = \Pi_1(\boldsymbol{u})\boldsymbol{u}_{2,\sigma} \end{cases} \tag{11}$$

Conversely, using (8) to eliminate γ from (9) we obtain an analogous equation on Ω_2:

$$\begin{cases} (\ddot{\boldsymbol{u}}_{2,\sigma}, N_{2,i})_{\Omega_2} + (\sigma(\boldsymbol{u}_2), \varepsilon(N_{2,i}))_{\Omega_2} = (\mathbf{f}, N_{2,i})_{\Omega_2} - \langle \Pi_2 \gamma_1(\ddot{\boldsymbol{u}}_{1,\sigma}, \boldsymbol{u}_1), N_{2,i} \rangle_\sigma & \forall i \in V(\sigma_2^h) \\ (\ddot{\boldsymbol{u}}_{2,0}, N_{2,i})_{\Omega_2} + (\sigma(\boldsymbol{u}_2), \varepsilon(N_{2,i}))_{\Omega_2} = (\mathbf{f}, N_{2,i})_{\Omega_2} & \forall i \in V(\breve{\Omega}_2^h) \\ \boldsymbol{u}_{2,\sigma} = \Pi_2(\boldsymbol{u}) \boldsymbol{u}_{1,\sigma} \end{cases} \tag{12}$$

Let $\vec{F}_i = (\vec{F}_{i,\sigma}, \vec{F}_{i,0})$ be the vector with elements

$$\vec{F}_i^k = (\mathbf{f}, N_{i,k})_{\Omega_i} - (\sigma(\boldsymbol{u}_i), \varepsilon(N_{i,k}))_{\Omega_i} \quad \forall k \in V(\Omega_i^h)\,. \tag{13}$$

Then, the interface equation in (11) can be written as

$$M_{1,\sigma} \ddot{\boldsymbol{u}}_{1,\sigma} = \vec{F}_{1,\sigma} + \overline{M}_{1,\sigma} P_1 \gamma_2(\ddot{\boldsymbol{u}}_{2,\sigma}, \boldsymbol{u}_2)\,, \tag{14}$$

whereas the matrix form of equation (10), which defines γ_2, is given by

$$\overline{M}_{2,\sigma} \gamma_2 = \vec{F}_{2,\sigma} - M_{2,\sigma} \ddot{\boldsymbol{u}}_{2,\sigma}\,.$$

Solving the latter for γ_2 yields

$$\gamma_2(\ddot{\boldsymbol{u}}_{2,\sigma}, \boldsymbol{u}_2) = \overline{M}_{2,\sigma}^{-1} \vec{F}_{2,\sigma} - \overline{M}_{2,\sigma}^{-1} M_{2,\sigma} \ddot{\boldsymbol{u}}_{2,\sigma}\,.$$

The algebraic form of (11) follows by substituting this result into (14):

$$\begin{cases} M_{1,\sigma}\, \ddot{\boldsymbol{u}}_{1,\sigma} + \overline{M}_{1,\sigma} P_1 \overline{M}_{2,\sigma}^{-1} M_{2,\sigma}\, \ddot{\boldsymbol{u}}_{2,\sigma} &=& \vec{F}_{1,\sigma} + \overline{M}_{1,\sigma} P_1 \overline{M}_{2,\sigma}^{-1} \vec{F}_{2,\sigma} \\ M_{1,0} \ddot{\boldsymbol{u}}_{1,0} &=& \vec{F}_{1,0} \\ \boldsymbol{u}_{1,\sigma} &=& P_1(\boldsymbol{u}) \boldsymbol{u}_{2,\sigma} \end{cases} \tag{15}$$

Proceeding along the same lines we obtain an analogous algebraic form for (11):

$$\begin{cases} M_{2,\sigma}\, \ddot{\boldsymbol{u}}_{2,\sigma} + \overline{M}_{2,\sigma} P_2 \overline{M}_{1,\sigma}^{-1} M_{1,\sigma}\, \ddot{\boldsymbol{u}}_{1,\sigma} &=& \vec{F}_{2,\sigma} + \overline{M}_{2,\sigma} P_2 \overline{M}_{1,\sigma}^{-1} \vec{F}_{1,\sigma} \\ M_{2,0} \ddot{\boldsymbol{u}}_{2,0} &=& \vec{F}_{2,0} \\ \boldsymbol{u}_{2,\sigma} &=& P_2(\boldsymbol{u}) \boldsymbol{u}_{1,\sigma} \end{cases} \tag{16}$$

4.4 Elimination of displacement continuity equations

Equations (15)–(16) remain coupled through their dependence on interface states from both subdomains. Under some additional assumptions on the matrix structure $P_i(\boldsymbol{u}_i)$ can be effectively approximated by the interface interpolant P_i in which case the weak continuity equations in (15)–(16) are replaced by

$$\boldsymbol{u}_{1,\sigma} = P_1 \boldsymbol{u}_{2,\sigma} \quad \text{and} \quad \boldsymbol{u}_{2,\sigma} = P_2 \boldsymbol{u}_{1,\sigma}\,, \tag{17}$$

respectively. The key factor that enables such an approximation is to work with diagonal mass matrices. Thus, from now on we assume that (i) assembly is performed using node-based quadrature rules, which result in

$$M_{i,\sigma} = diag(m^k_{i,\sigma}) \quad \text{and} \quad \overline{M}_{i,\sigma} = diag(\overline{m}^k_{i,\sigma}); \quad i = 1, 2\,,$$

and (ii) displacement continuity conditions are given by (17). For clarity we explain elimination of interface states in a two-dimensional setting. In this case matrix forms of interface transfer operators Π_i assume a particularly simple form with at most two non-zero elements per row. We explain the structure of P_1. Let $\boldsymbol{x}_{1,i} \in \sigma^h_1$ be an arbitrary vertex on the interface of Ω_1 and $K_{2,k_i} \in \sigma^h_2$ be the element from the interface of Ω_2, which contains[2] $\boldsymbol{x}_{1,i}$. Since σ is one-dimensional, element K_{2,k_i} is an interval with endpoints $\boldsymbol{x}_{2,k_i-1}$ and $\boldsymbol{x}_{2,k_i}$, respectively. As a result, (1) reduces to the following sum

$$\sum_{k\in V(K_{2,k_i})} \vec{\boldsymbol{u}}^k_{2,\sigma} N_{2,k}(\boldsymbol{x}_{1,i}) = \vec{\boldsymbol{u}}^{k_i-1}_{2,\sigma} N_{2,k_i-1}(\boldsymbol{x}_{1,i}) + \vec{\boldsymbol{u}}^{k_i}_{2,\sigma} N_{2,k_i}(\boldsymbol{x}_{1,i}) \tag{18}$$

Since basis functions form a partition of unity on every element, $N_{2,k_i-1}(\boldsymbol{x}_{1,i})+N_{2,k_i}(\boldsymbol{x}_{1,i}) = 1$ and so, there exists $0 \le \alpha_i \le 1$ such that $N_{2,k_i-1}(\boldsymbol{x}_{1,i}) = \alpha_{1,i}$ and $N_{2,k_i}(\boldsymbol{x}_{1,i}) = 1 - \alpha_{1,i}$ It follows that the matrix P_1 is given by

$$(P_1)_{ij} = \begin{cases} \alpha_{1,i} & \text{if } j = k_i - 1 \\ 1 - \alpha_{1,i} & \text{if } j = k_i \\ 0 & \text{otherwise} \end{cases} \tag{19}$$

where $K_{2,k_i} = [\boldsymbol{x}_{2,k_i-1}, \boldsymbol{x}_{2,k_i}]$ is the element from the interface on Ω_2 containing vertex $\boldsymbol{x}_{1,i}$ from the interface on Ω_1. Repeating the same arguments for Π_2 shows that

$$(P_2)_{ij} = \begin{cases} \alpha_{2,i} & \text{if } j = k_i - 1 \\ 1 - \alpha_{2,i} & \text{if } j = k_i \\ 0 & \text{otherwise} \end{cases} \tag{20}$$

where $K_{1,k_i} = [\boldsymbol{x}_{1,k_i-1}, \boldsymbol{x}_{1,k_i}]$ is the element from the interface on Ω_1 containing vertex $\boldsymbol{x}_{2,i}$ from the interface on Ω_2 and $\alpha_{2,i} = N_{1,k_i-1}(\boldsymbol{x}_{2,i})$ and $1 - \alpha_{2,i} = N_{1,k_i}(\boldsymbol{x}_{2,i})$.

Since interior equations are fully decoupled from the interface equations we focus solely on the structure of the latter. Their right hand sides are given by

$$\left(\vec{F}_{1,\sigma} + \overline{M}_{1,\sigma} P_1 \overline{M}^{-1}_{2,\sigma} \vec{F}_{2,\sigma}\right)_j = F^j_{1,\sigma} + \overline{m}^j_{1,\sigma}\left[\alpha_{1,j}\frac{F^{k_j-1}_{2,\sigma}}{\overline{m}^{k_j-1}_{2,\sigma}} + (1-\alpha_{1,j})\frac{F^{k_j}_{2,\sigma}}{\overline{m}^{k_j}_{2,\sigma}}\right]$$

[2]If $\boldsymbol{x}_{1,i}$ is also a vertex in σ^h_2, then it is shared by two elements in σ^2_h. In this case we can take K_{2,k_i} to be either one of these two elements.

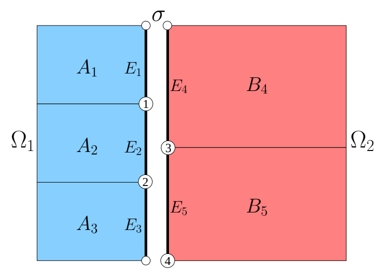

Figure 1: Assumption (23) holds provided $(A_1 + A_2)/(A_2 + A_3) \approx (E_1 + E_2)/(E_2 + E_3)$ and $(B_4 + B_5)/B_5 \approx (E_4 + E_5)/E_5$.

for the interface equation on Ω_1 and

$$\left(\vec{F}_{2,\sigma} + \overline{M}_{2,\sigma} P_2 \overline{M}_{1,\sigma}^{-1} \vec{F}_{1,\sigma}\right)_j = F_{2,\sigma}^j + \overline{m}_{2,\sigma}^j \left[\alpha_{2,j} \frac{F_{1,\sigma}^{k_j-1}}{\overline{m}_{1,\sigma}^{k_j-1}} + (1-\alpha_{2,j}) \frac{F_{1,\sigma}^{k_j}}{\overline{m}_{1,\sigma}^{k_j}}\right],$$

for the interface equation on Ω_2.

Consider the terms involving displacements from the opposite sides of the interface, that is, $\overline{M}_{1,\sigma} P_1 \overline{M}_{2,\sigma}^{-1} M_{2,\sigma} \ddot{\boldsymbol{u}}_{2,\sigma}$ in (15) and $\overline{M}_{2,\sigma} P_2 \overline{M}_{1,\sigma}^{-1} M_{1,\sigma} \ddot{\boldsymbol{u}}_{1,\sigma}$ in (16). We have that

$$\left(\overline{M}_{1,\sigma} P_1 \overline{M}_{2,\sigma}^{-1} M_{2,\sigma} \ddot{\boldsymbol{u}}_{2,\sigma}\right)_j = \overline{m}_{1,\sigma}^j \left[\alpha_{1,j} \frac{m_{2,\sigma}^{k_j-1}}{\overline{m}_{2,\sigma}^{k_j-1}} \ddot{\boldsymbol{u}}_{2,\sigma}^{k_j-1} + (1-\alpha_{1,j}) \frac{m_{2,\sigma}^{k_j}}{\overline{m}_{2,\sigma}^{k_j}} \ddot{\boldsymbol{u}}_{2,\sigma}^{k_j}\right] \tag{21}$$

and

$$\left(\overline{M}_{2,\sigma} P_2 \overline{M}_{1,\sigma}^{-1} M_{1,\sigma} \ddot{\boldsymbol{u}}_{1,\sigma}\right)_j = \overline{m}_{2,\sigma}^j \left[\alpha_{2,j} \frac{m_{1,\sigma}^{k_j-1}}{\overline{m}_{1,\sigma}^{k_j-1}} \ddot{\boldsymbol{u}}_{1,\sigma}^{k_j-1} + (1-\alpha_{2,j}) \frac{m_{1,\sigma}^{k_j}}{\overline{m}_{1,\sigma}^{k_j}} \ddot{\boldsymbol{u}}_{1,\sigma}^{k_j}\right]. \tag{22}$$

For shape-regular grids it is not unreasonable to expect that (see Fig.2)

$$\frac{m_{2,\sigma}^{k_j-1}}{\overline{m}_{2,\sigma}^{k_j-1}} \approx \frac{m_{2,\sigma}^{k_j}}{\overline{m}_{2,\sigma}^{k_j}} := \mu_{2,\sigma}^j \quad \text{and} \quad \frac{m_{1,\sigma}^{k_j-1}}{\overline{m}_{1,\sigma}^{k_j-1}} \approx \frac{m_{1,\sigma}^{k_j}}{\overline{m}_{1,\sigma}^{k_j}} := \mu_{1,\sigma}^j\,. \tag{23}$$

This allows us to exchange the order of interpolation and matrix multiplication in (21):

$$\left(\overline{M}_{1,\sigma} P_1 \overline{M}_{2,\sigma}^{-1} M_{2,\sigma} \ddot{\boldsymbol{u}}_{2,\sigma}\right)_j = \overline{m}_{1,\sigma}^j \mu_{2,\sigma}^j \left[\alpha_{1,j} \ddot{\boldsymbol{u}}_{2,\sigma}^{k_j-1} + (1-\alpha_{1,j}) \ddot{\boldsymbol{u}}_{2,\sigma}^{k_j}\right] = \overline{m}_{1,\sigma}^j \mu_{2,\sigma}^j (P_1 \ddot{\boldsymbol{u}}_{2,\sigma})_j.$$

Likewise, exchanging the order of operators in (22) gives

$$\left(\overline{M}_{2,\sigma} P_2 \overline{M}_{1,\sigma}^{-1} M_{1,\sigma} \ddot{\boldsymbol{u}}_{1,\sigma}\right)_j = \overline{m}_{2,\sigma}^j \mu_{1,\sigma}^j \left[\alpha_{2,j} \ddot{\boldsymbol{u}}_{1,\sigma}^{k_j-1} + (1-\alpha_{2,j}) \ddot{\boldsymbol{u}}_{1,\sigma}^{k_j}\right] = \overline{m}_{2,\sigma}^j \mu_{1,\sigma}^j (P_2 \ddot{\boldsymbol{u}}_{1,\sigma})_j\,.$$

From (17) it follows that $\ddot{\boldsymbol{u}}_{1,\sigma}^j = (P_1 \ddot{\boldsymbol{u}}_{2,\sigma})_j$ and $\ddot{\boldsymbol{u}}_{2,\sigma}^j = (P_2 \ddot{\boldsymbol{u}}_{1,\sigma})_j$. Using these identities we can eliminate $\ddot{\boldsymbol{u}}_{2,\sigma}$ from (21) and $\ddot{\boldsymbol{u}}_{1,\sigma}$ from (22) to obtain

$$\left(\overline{M}_{1,\sigma} P_1 \overline{M}_{2,\sigma}^{-1} M_{2,\sigma}\right) \ddot{\boldsymbol{u}}_{2,\sigma} \approx \left(\overline{M}_{1,\sigma} \mu_{2,\sigma}\right) \ddot{\boldsymbol{u}}_{1,\sigma}$$

and

$$\left(\overline{M}_{2,\sigma} P_2 \overline{M}_{1,\sigma}^{-1} M_{1,\sigma} \ddot{\boldsymbol{u}}_{1,\sigma}\right) \approx \left(\overline{M}_{2,\sigma} \mu_{1,\sigma}\right) \ddot{\boldsymbol{u}}_{2,\sigma} \,,$$

respectively. This decouples (15)–(16) into an independent equation

$$\left\{ \begin{array}{rcl} \left(M_{1,\sigma} + \overline{M}_{1,\sigma}\mu_{2,\sigma}\right) \ddot{\boldsymbol{u}}_{1,\sigma} & = & \vec{F}_{1,\sigma} + \overline{M}_{1,\sigma} P_1 \overline{M}_{2,\sigma}^{-1} \vec{F}_{2,\sigma} \\ M_{1,0}\, \ddot{\boldsymbol{u}}_{1,0} & = & \vec{F}_{1,0} \end{array} \right. \tag{24}$$

on Ω_1, and another independent subdomain equation

$$\left\{ \begin{array}{rcl} \left(M_{2,\sigma} + \overline{M}_{2,\sigma}\mu_{1,\sigma}\right) \ddot{\boldsymbol{u}}_{2,\sigma} & = & \vec{F}_{2,\sigma} + \overline{M}_{2,\sigma} P_2 \overline{M}_{1,\sigma}^{-1} \vec{F}_{1,\sigma} \\ M_{2,0} \ddot{\boldsymbol{u}}_{2,0} & = & \vec{F}_{2,0} \end{array} \right. \tag{25}$$

on Ω_2. The interface equations in each subdomain have the following component form:

$$\left(m_{1,\sigma}^j + \overline{m}_{1,\sigma}^j \mu_{2,\sigma}^j\right) \ddot{\boldsymbol{u}}_{1,\sigma}^j = F_{1,\sigma}^j + \overline{m}_{1,\sigma}^j \left[\alpha_{1,j} \frac{F_{2,\sigma}^{k_j-1}}{\overline{m}_{2,\sigma}^{k_j-1}} + (1-\alpha_{1,j}) \frac{F_{2,\sigma}^{k_j}}{\overline{m}_{2,\sigma}^{k_j}}\right]; \quad j \in V(\sigma_1^h) \tag{26}$$

and

$$\left(m_{2,\sigma}^j + \overline{m}_{2,\sigma}^j \mu_{1,\sigma}^j\right) \ddot{\boldsymbol{u}}_{2,\sigma}^j = F_{2,\sigma}^j + \overline{m}_{2,\sigma}^j \left[\alpha_{2,j} \frac{F_{1,\sigma}^{k_j-1}}{\overline{m}_{1,\sigma}^{k_j-1}} + (1-\alpha_{2,j}) \frac{F_{1,\sigma}^{k_j}}{\overline{m}_{1,\sigma}^{k_j}}\right]; \quad j \in V(\sigma_2^h). \tag{27}$$

Modification of subdomain mass matrices in (26)–(27) can be interpreted as their completion to bulk mass matrices on $S_{1,\sigma}^h \cup S_{2,\sigma}^h$.

4.5 Fully discrete partitioned equations

We discretize (26)–(27) in time using second central difference

$$\ddot{\boldsymbol{u}}_i(t,\boldsymbol{x}) \approx \frac{\boldsymbol{u}_i(t+\Delta t,\boldsymbol{x}) - 2\boldsymbol{u}_i(t,\boldsymbol{x}) + \boldsymbol{u}_i(t-\Delta t,\boldsymbol{x})}{\Delta t^2} \,.$$

Let $\boldsymbol{u}_i^{n+1} \in S_i^h$, $\boldsymbol{u}_i^n \in S_i^h$ and $\boldsymbol{u}_i^{n-1} \in S_i^h$ denote finite element approximations of $\boldsymbol{u}_i$ at $t_n + \Delta t$, t_n, and $t_{n-1} = t_n - \Delta t$, respectively, $\ddot{D}^{n+1}(\boldsymbol{u}_i) = (\boldsymbol{u}_i^{n+1} - 2\boldsymbol{u}_i^n + \boldsymbol{u}_i^{n-1})/\Delta t^2$, and $(\vec{F}_i)^n$ be the force vector (13) evaluated at $\boldsymbol{u}_i^n$. Then, for given $\boldsymbol{u}_i^n$ and $\boldsymbol{u}_i^{n-1}$, the fully discrete partitioned formulation is to find $\boldsymbol{u}_1^{n+1}$ such that

$$\left\{ \begin{array}{rcl} \left(M_{1,\sigma} + \overline{M}_{1,\sigma}\mu_{2,\sigma}\right) \ddot{D}^{n+1}(\boldsymbol{u}_{1,\sigma}) & = & (\vec{F}_{1,\sigma})^n + \overline{M}_{1,\sigma} P_1 \overline{M}_{2,\sigma}^{-1} (\vec{F}_{2,\sigma})^n \\ M_{1,0} \ddot{D}^{n+1}(\boldsymbol{u}_{1,0}) & = & (\vec{F}_{1,0})^n \end{array} \right. \tag{28}$$

and $\boldsymbol{u}_2^{n+1}$ such that

$$\left\{ \begin{array}{rcl} \left(M_{2,\sigma} + \overline{M}_{2,\sigma}\mu_{1,\sigma}\right) \ddot{D}^{n+1}(\boldsymbol{u}_{2,\sigma}) & = & (\vec{F}_{2,\sigma})^n + \overline{M}_{2,\sigma} P_2 \overline{M}_{1,\sigma}^{-1} (\vec{F}_{1,\sigma})^n \\ M_{2,0} \ddot{D}^{n+1}(\boldsymbol{u}_{2,0}) & = & (\vec{F}_{2,0})^n \end{array} \right. \tag{29}$$

for the finite element approximations $\boldsymbol{u}_i^{n+1}$, $i = 1, 2$ of the subdomain solutions at t_{n+1}.

5 Equivalence to a monolithic discretization on matching interface grids

If Ω_1^h and Ω_2^h are such that interface grids match then $\Omega_1 \cup \Omega_2$ is a conforming partition of Ω and $S^h = S_1^h \cup S_2^h$ is a conforming finite element subspace of $\mathbf{H}^1(\Omega)$. The corresponding monolithic formulation of (2) is

$$M\ddot{D}^{n+1}\boldsymbol{v} = (\vec{F})^n\,.$$

where M and $\vec{F}$ are a diagonal mass matrix and force vector assembled using S^h. Partitioning of mesh nodes into interface and subdomain nodes induces partitioning of the solution vector $\boldsymbol{v}$ into coefficient vectors $\boldsymbol{v}_\sigma$, $\boldsymbol{v}_{1,0}$ and $\boldsymbol{v}_{2,0}$ corresponding to interface and interior subdomain nodes, respectively. As a result, we can write the monolithic problem in the following block diagonal form:

$$\left\{\begin{array}{rcl} M_\sigma \ddot{D}^{n+1}(\boldsymbol{v}_\sigma) & = & (\vec{F}_\sigma)^n \\ M_{1,0}\ddot{D}^{n+1}(\boldsymbol{v}_{1,0}) & = & (\vec{F}_{1,0})^n \\ M_{2,0}\ddot{D}^{n+1}(\boldsymbol{v}_{2,0}) & = & (\vec{F}_{2,0})^n \end{array}\right. \tag{30}$$

Theorem 1 *Assume that interface grids σ_1^h and σ_2^h are matching and interface displacements at all previous time steps coincide:*

$$(\vec{\boldsymbol{u}}_{1,\sigma})^\nu = (\vec{\boldsymbol{u}}_{2,\sigma})^\nu \quad \nu = 1, 2, \ldots, n-1, n\,. \tag{31}$$

Then the partitioned solution $(\vec{\boldsymbol{u}}_{1,\sigma}, \vec{\boldsymbol{u}}_{1,0})^{n+1}$, $(\vec{\boldsymbol{u}}_{2,\sigma}, \vec{\boldsymbol{u}}_{2,0})^{n+1}$ coincides with the solution $\vec{\boldsymbol{v}}^{n+1} = (\vec{\boldsymbol{v}}_\sigma, \vec{\boldsymbol{v}}_{1,0}, \vec{\boldsymbol{v}}_{2,0})^{n+1}$ of the monolithic problem: $\vec{\boldsymbol{v}}_\sigma^{n+1} = \vec{\boldsymbol{u}}_{1,\sigma}^{n+1} = \vec{\boldsymbol{u}}_{2,\sigma}^{n+1}$, $\vec{\boldsymbol{u}}_{1,0}^{n+1} = \vec{\boldsymbol{v}}_{1,0}^{n+1}$ and $\vec{\boldsymbol{u}}_{2,0}^{n+1} =, \vec{\boldsymbol{v}}_{2,0}^{n+1}$.

Proof. For clarity we present the proof for the two-dimensional formulation (24)–(25) and skip the time step index. Owing to the assumption that interface grids on Ω_1 and Ω_2 match, it follows that the area mass matrices $\overline{M}_{1,\sigma}$ and $\overline{M}_{2,\sigma}$ are identical, i.e., they have the same dimension and with proper renumbering of their elements we can write

$$\overline{m}_{1,\sigma}^j = \overline{m}_{2,\sigma}^j \qquad \forall j \in V(\sigma_1^h) \equiv V(\sigma_2^h)$$

For matching interface grids we also have that $P_1 = P_1 = I$. As a result, the interface equations assume the form

$$\left(m_{1,\sigma}^j + m_{2,\sigma}^j\right)\boldsymbol{u}_{1,\sigma}^j = F_{1,\sigma}^j + F_{2,\sigma}^j \qquad \forall j \in V(\sigma_1^h)$$

and

$$\left(m_{2,\sigma}^j + m_{1,\sigma}^j\right)\boldsymbol{u}_{2,\sigma}^j = F_{2,\sigma}^j + F_{1,\sigma}^j \qquad \forall j \in V(\sigma_2^h),$$

respectively. Thus, for matching interface grids (28)–(29) has the form

$$\left\{\begin{array}{rcl} (M_{1,\sigma} + M_{2,\sigma})\vec{\boldsymbol{u}}_{1,\sigma} & = & \vec{F}_{1,\sigma} + \vec{F}_{2,\sigma} \\ M_{1,0}\vec{\boldsymbol{u}}_{1,0} & = & \vec{F}_{1,0} \end{array}\right. ; \quad \left\{\begin{array}{rcl} (M_{2,\sigma} + M_{1,\sigma})\vec{\boldsymbol{u}}_{2,\sigma} & = & \vec{F}_{2,\sigma} + \vec{F}_{1,\sigma} \\ M_{2,0}\vec{\boldsymbol{u}}_{2,0} & = & \vec{F}_{2,0} \end{array}\right. . \tag{32}$$

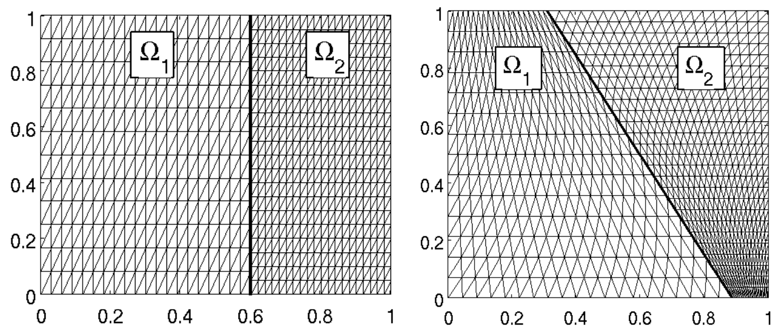

Figure 2: Left: uniform partitions of Ω_1 and Ω_2 into triangles with a vertical interface at $x = 0.6$ *cm*. Right: nonuniform partitions of Ω_1 and Ω_2 into triangles with an interface having a slope of tan(110°) and passing through (0.6,0.5).

It immediately follows that $\vec{\boldsymbol{u}}_{1,0} = \vec{\boldsymbol{v}}_{1,0}$ and $\vec{\boldsymbol{u}}_{2,0} = \vec{\boldsymbol{v}}_{2,0}$. On the other hand, it is easy to see that for matching interface partitions, the monolithic volume interface mass matrix is sum of the volume interface mass matrices on Ω_1 and Ω_2, i.e., $M_\sigma = M_{1,\sigma} + M_{2,\sigma}$. Furthermore, if (31) holds, a direct calculation shows that the monolithic interface force vector is sum of the interface force vectors on Ω_1 and Ω_2: $\vec{F}_\sigma = \vec{F}_{1,\sigma} + \vec{F}_{2,\sigma}$. Therefore, $\vec{\boldsymbol{u}}_{1,\sigma}$ and $\vec{\boldsymbol{u}}_{2,\sigma}$ solve an identical equation, which coincides with the monolithic interface equation and so, $\vec{\boldsymbol{u}}_{1,\sigma} = \vec{\boldsymbol{u}}_{2,\sigma} = \vec{\boldsymbol{v}}_\sigma$. □

6 Convergence rates

We use the manufactured solution

$$\boldsymbol{u} = \Big(\sin(5\pi x)\cos(3\pi y)\log(1+t); 4x^4\cos(4\pi y)\sqrt{t+2}\Big)^T \tag{33}$$

to estimate numerical convergence rates of the algorithm. We assume linear homogenous isotropic solid with $\mu = 0.01$, $\lambda = 0.02$ $dyne/cm^2$ and density 1 g/cm^3. Substitution of (35) into the governing equations yields the problem data. The domain $\Omega = [0,1]^2$ is divided into two subdomains using a vertical and a slanted interface; see Fig. 3. Each subdomain is meshed independently and the interface grids are non matching.

	Error/Rate		
Mesh 1	12×20	24×40	48×80
Mesh 2	20×20	40×40	80×80
$\\|\boldsymbol{u} - \boldsymbol{u}_1^h\\|_{0,\Omega_1}$	7.97e-03/-	2.06e-03/1.95	5.12e-04/2.01
$\\|\boldsymbol{u} - \boldsymbol{u}_2^h\\|_{0,\Omega_2}$	2.58e-02/-	6.42e-03/2.01	1.59e-03/2.01
$\\|\boldsymbol{u} - \boldsymbol{u}_1^h\\|_{1,\Omega_1}$	5.61e-01/-	2.59e-01/1.11	1.30e-01/1.00
$\\|\boldsymbol{u} - \boldsymbol{u}_2^h\\|_{1,\Omega_2}$	2.11e+00/-	1.06e+00/1.00	5.29e-01/1.00

Table 1: Errors and convergence rates using a vertical interface and uniform meshes at $t = 0.25$ *s*.

	Error/Rate			
Mesh 1	14×20	28×40	56×80	48×80
Mesh 2	26×20	52×40	104×80	48×80
$\\|\boldsymbol{u} - \boldsymbol{u}_1^h\\|_{0,\Omega_1}$	8.19e-03/-	2.07e-03/1.98	5.16e-04/2.01	1.37e-04/1.92
$\\|\boldsymbol{u} - \boldsymbol{u}_2^h\\|_{0,\Omega_2}$	1.52e-02/-	3.79e-03/2.00	9.58e-04/1.99	2.48e-04/1.95
$\\|\boldsymbol{u} - \boldsymbol{u}_1^h\\|_{1,\Omega_1}$	5.64e-01/-	2.78e-01/1.02	1.39e-01/1.00	6.94e-02/1.00
$\\|\boldsymbol{u} - \boldsymbol{u}_2^h\\|_{1,\Omega_2}$	1.63e+00/-	8.22e-01/0.99	4.12e-01/1.00	2.06e-01/1.00

Table 2: Errors and convergence rates using a slanted interface and non uniform meshes at $t = 0.25\ s$.

We observe in Tables 1 and 2 that by using a coincidental interface with nonmatching vertices and temporal step sizes on the order of h, the rate of convergence is second order regardless of the interface orientation.

6.1 Equivalence to a monolithic solution for matching interface grids

To confirm numerically Theorem **??** we use the same interface configurations as before, but consider grids with matching interface nodes. In this case the union $\Omega_1^h \cup \Omega_h^2$ defines a conforming mesh partition of Ω. The difference in solutions, shown in Table 3, left, are

Interface	Vertical	Slanted
Mesh 1	24×20	24×20
Mesh 2	24×20	24×20
$\\|\boldsymbol{u_1}^h - \boldsymbol{u}^h\\|_{0,\Omega_1}$	3.38e-17	9.43e-17
$\\|\boldsymbol{u_2}^h - \boldsymbol{u}^h\\|_{0,\Omega_2}$	1.07e-15	1.05e-15
$\\|\boldsymbol{u_1}^h - \boldsymbol{u}^h\\|_{1,\Omega_1}$	2.49e-15	7.74e-15
$\\|\boldsymbol{u_2}^h - \boldsymbol{u}^h\\|_{1,\Omega_2}$	9.92e-14	1.23e-13

Interface	Vertical	Slanted
Mesh 1	6×3	6×3
Mesh 2	34×11	34×11
$\\|\boldsymbol{u} - \boldsymbol{u}_1^h\\|_{0,\Omega_1}$	3.45e-15	3.54e-15
$\\|\boldsymbol{u} - \boldsymbol{u}_2^h\\|_{0,\Omega_2}$	4.00e-15	4.11e-15
$\\|\boldsymbol{u} - \boldsymbol{u}_1^h\\|_{1,\Omega_1}$	1.16e-14	1.59e-14
$\\|\boldsymbol{u} - \boldsymbol{u}_2^h\\|_{1,\Omega_2}$	6.42e-14	7.85e-14

Table 3: Left: Comparison of the monolithic solution $\boldsymbol{u}^h$ with subdomain solutions $\boldsymbol{u}_1^h$ and $\boldsymbol{u}_2^h$. Right: patch test errors at time $t = 0.05\ s$

equivalent up to roundoff whether computed through the monolithic formulation or using the algorithm based on variational flux recovery.

6.2 Preservation of linear displacements

The patch test [7] requires a method to recover a certain class of solutions. This section verifies that our method is capable of reproducing linear displacement fields exactly. We consider $\Omega = [-1, 1]^2$ with a vertical and a slanted interface and non matching interface grids; see Fig.5. The exact solution is

$$\boldsymbol{u} = (-5x + 50y, 33x - 22y) \tag{34}$$

We assume linear homogenous isotropic solid with $\mu = 1.5$, $\lambda = 7\ dyne/cm^2$ and density $1\ g/cm^3$. As before, substitution of (36) into the governing equations yields the problem data. Table 3, right, confirms that the new algorithm recovers the linear displacement field up to machine precision, i.e., it passes a patch test for non matching interface grids.

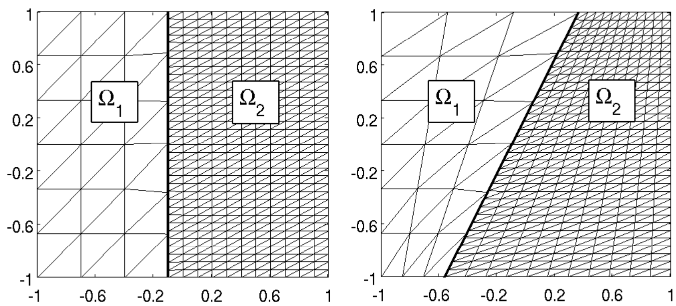

Figure 3: Uniform and non uniform domain discretizations on which to recover a linear solution.

7 CONCLUSIONS

We have presented a new explicit method for elastodynamic problems with interfaces, which enables partitioned solution of the equations. Numerical studies show that the method passes a linear patch test and is second order accurate. If the interface grids have matching nodes then the method recovers a solution of the monolithic discretization.

REFERENCES

[1] R. Becker, E. Burman, and P. Hansbo, *A Nitsche extended finite element method for incompressible elasticity with discontinuous modulus of elasticity*, Computer Methods in Applied Mechanics and Engineering, 198 (2009), pp. 3352 – 3360.

[2] G. Carey, S. Chow, and M. Seager, *Approximate boundary-flux calculations*, Computer Methods in Applied Mechanics and Engineering, 50 (1985), pp. 107 – 120.

[3] A. Hansbo and P. Hansbo, *An unfitted finite element method, based on nitsche's method, for elliptic interface problems*, Computer Methods in Applied Mechanics and Engineering, 191 (2002), pp. 5537 – 5552.

[4] ——, *A finite element method for the simulation of strong and weak discontinuities in solid mechanics*, Computer Methods in Applied Mechanics and Engineering, 193 (2004), pp. 3523 – 3540.

[5] R. Kramer, P. Bochev, C. Siefert, and T. Voth, *An extended finite element method with algebraic constraints (XFEM-AC) for problems with weak discontinuities*, Computer Methods in Applied Mechanics and Engineering, 266 (2013), pp. 70 – 80.

[6] T. Lin, D. Sheen, and X. Zhang, *A locking-free immersed finite element method for planar elasticity interface problems*, Journal of Computational Physics, 247 (2013), pp. 228 – 247.

[7] R. L. Taylor, J. C. Simo, O. C. Zienkiewicz, and A. C. H. Chan, *The patch test—a condition for assessing fem convergence*, International Journal for Numerical Methods in Engineering, 22 (1986), pp. 39–62.